Novel Modal Approximation Scheme for Plasmonic Transmission Problems

Gerhard Unger, Andreas Trügler, and Ulrich Hohenester*
Institute of Physics, University of Graz, Universitätsplatz 5, 8010 Graz, Austria

(Received 15 May 2018; published 14 December 2018)

The concept of resonances and modes for the description of particle plasmons has recently received great interest, both in the context of efficient simulations as well as for an intuitive interpretation in physical terms. While resonance modes have been successfully employed for geometries whose optical response is governed by a few modes only, the resonance mode description exhibits considerable difficulties for larger nanoparticles with their richer mode spectra. We analyze the problem using a boundary element method approach together with a Mie solution for spherical particles, and identify the fixed link between the electric and magnetic components of the resonance modes as the main source for this shortcoming. We suggest a novel modal approximation scheme that allows us in principle to overcome this problem.

DOI: 10.1103/PhysRevLett.121.246802

Plasmonics allows light confinement at the nanoscale [1–3]: light is bound to coherent charge oscillations at the interface between a metallic nanoparticle and an embedding dielectric, so-called particle plasmons, which come together with strong and localized electromagnetic fields in the vicinity of the particles [4]. The optical spectra of plasmonic nanoparticles are usually governed by a few resonance modes only, and one often seeks for a theoretical description in terms of such modes instead of solving the full Maxwell equations.

For sufficiently small nanoparticles one can employ the quasistatic approximation where it becomes possible to define so-called geometric eigenmodes [5–7] which can be combined with the material properties to obtain a simple, flexible, and intuitive description scheme widely used in the field of plasmonics. For instance, plasmon field tomography [8,9] and self-hybridization of non-Hermitian plasmonic systems [10] have been demonstrated within such an approach. Things are less obvious for the full Maxwell equations since it is no longer possible to disentangle geometric and material properties. The standard procedure for defining resonance modes in this case is by means of so-called quasinormal modes [11], which have been successfully employed for plasmonic nanoparticles whose optical response is governed by a few modes only [12–16]. We also mention the resonant state expansion method, where resonance modes of a reference geometry are used for the expansion of a deformed geometry and perturbed material parameters [17,18], and the computation of resonace modes for fixed frequencies [19].

In this Letter we investigate the framework of resonance modes for larger nanoparticles with pronounced plasmon peaks, however, with richer resonance spectra in comparison to small particles. We developed and implemented an efficient and robust numerical computation scheme for resonance modes based on the boundary element method (BEM)which is interesting in its own right but not essential for our findings that could have been obtained equally well from other numerical schemes, such as the finite element (FEM) [12–14] or finite difference time domain (FDTD) [15,16] methods. Most importantly, we observe that even for nanoparticles of moderate size there are significant differences between full simulation results and those based on resonance modes. To evaluate whether these discrepancies are due to (i) a too small number of resonance modes or (ii) a too simple prescription for the computation of the expansion coefficients, we analyze the problem for spherical particles within the framework of Mie theory. We find that the major shortcoming is the description of electric and magnetic field contributions using a single, combined expansion coefficient, which only works for small particles but becomes in general questionable for larger ones. To overcome this problem, we suggest a novel approximation scheme with separate coefficients for the electric and magnetic field components, which provides excellent agreement with full simulations even for larger nanoparticles.

Boundary integral formulation.—To set the stage for our following discussion, we briefly review the basic ingredients of our boundary integral method approach. We consider a nanoparticle with domain Ω_1 that is separated by a sharp boundary $\Gamma := \partial\Omega_1$ from the embedding medium $\Omega_2 := \mathbb{R}^3 \backslash (\Omega_1 \cup \Gamma)$. Additionally, we assume homogeneous permittivities and permeabilities ϵ_1, μ_1 inside and ϵ_2, μ_2 outside the particle. The solution $(\mathbf{E}, \mathbf{H})$ of the transmission problem, where the nanoparticle's response is computed for some incoming fields, has to satisfy Maxwell equations in Ω_1 and Ω_2, as well as the Silver-Müller radiation condition of outgoing waves at infinity. The total fields $(\mathbf{E}, \mathbf{H})$ can be represented by the Stratton-Chu formula in terms of the tangential fields on the interface Γ,

$$\mathbf{e} := \mathbf{E}|_\Gamma \times \mathbf{n}, \qquad \mathbf{h} := \mathbf{H}|_\Gamma \times \mathbf{n}, \tag{1}$$

where $\mathbf{n}$ denotes the unit normal vector field on the interface pointing into Ω_2. We use the Poggio-Miller-Chang-Harrington-Wu-Tsai formulation [20–22] for the boundary integral formulation of the transmission and resonance problem. A rigorous mathematical analysis of this formulation and its numerical approximation for general Lipschitz domains was presented for the transmission problem in Refs. [23,24] and for the resonance problem in Ref. [25]. See also the Supplemental Material (SM) [26] for more details. The unknown fields $\mathbf{e}$, $\mathbf{h}$ on the boundary can then be determined by solving the 2×2 block boundary integral operator equation [see also Eq. (13) of SM [26]]

$$\mathcal{A}(\omega)\begin{pmatrix}\mathbf{e}\\ \mathbf{h}\end{pmatrix} = \begin{pmatrix}\mathbf{e}^{\mathrm{inc}}\\ \mathbf{h}^{\mathrm{inc}}\end{pmatrix}, \tag{2}$$

where $(\mathbf{e}^{\mathrm{inc}}, \mathbf{h}^{\mathrm{inc}})$ are the tangential components of the incident fields on the interface Γ.

Resonance modes.—In this Letter we seek to approximate the solution of Eq. (2) using the concept of resonance modes. We call a frequency $\omega_j \in \mathbb{C}$ a resonance and nonzero fields $(\mathbf{e}_j, \mathbf{h}_j)$ a corresponding mode if

$$\mathcal{A}(\omega_j)\begin{pmatrix}\mathbf{e}_j\\ \mathbf{h}_j\end{pmatrix} = \begin{pmatrix}\mathbf{0}\\ \mathbf{0}\end{pmatrix}. \tag{3}$$

Note that the resonance problem of Eq. (3) is a nonlinear eigenvalue problem with respect to the eigenvalue parameter ω. It fits in the framework of eigenvalue problems for holomorphic Fredholm operator-valued functions [29,30], which is the basis of our analysis. Below we will present a powerful scheme based on a contour integral method [31] that allows us to efficiently compute all resonance modes within a given region of the complex plane. For the moment, we assume that ω_j and the corresponding eigenmodes are known. The central idea of the resonance mode framework is to expand the solution of the transmission problem, Eq. (2), in terms of a few representative modes through

$$\begin{pmatrix}\mathbf{e}\\ \mathbf{h}\end{pmatrix} \approx \sum_{j=1}^{J} \alpha_j(\omega)\begin{pmatrix}\mathbf{e}_j\\ \mathbf{h}_j\end{pmatrix}, \tag{4}$$

and to compute the expansion coefficients using some suitable prescription to be discussed below. To provide a viable scheme, the number of modes J needed to give a reasonable approximation should be sufficiently small. This has been demonstrated for plasmonic nanoparticles using FEM [12–14] and FDTD [16] simulations.

In what follows we present two schemes for the computation of $\alpha_j(\omega)$. The first one is a Galerkin scheme where we consider the approximate solution of the transmission problem in the space

$$\mathcal{U} := \mathrm{span}\{\mathfrak{u}_j : j = 1, \ldots, J\}, \qquad \mathfrak{u}_j := \begin{pmatrix}\mathbf{e}_j\\ \mathbf{h}_j\end{pmatrix},$$

and use the same space for the testing functions. The Galerkin approximation $\mathfrak{u}^{\mathrm{G}} = \sum_{j=1}^{J} \alpha_j^G(\omega)\mathfrak{u}_j$ is then obtained from a variational principle that seeks for the "best" expansion coefficients $\alpha_j^G(\omega)$ which satisfy the system of J linear equations,

$$\sum_{j=1}^{J} \alpha_j^{\mathrm{G}}(\omega)\langle \mathcal{A}(\omega)\mathfrak{u}_j, \overline{\mathfrak{u}_\ell}\rangle = \langle \mathfrak{u}^{\mathrm{inc}}, \overline{\mathfrak{u}_\ell}\rangle, \qquad \ell = 1, \ldots, J, \tag{5}$$

where $\bar{\cdot}$ denotes complex conjugation and the pairing is defined by

$$\left\langle \begin{pmatrix}\mathbf{f}_1\\ \mathbf{f}_2\end{pmatrix}, \begin{pmatrix}\mathbf{g}_1\\ \mathbf{g}_2\end{pmatrix} \right\rangle := \langle \mathbf{f}_1, \mathbf{g}_2\rangle_\Gamma + \langle \mathbf{f}_2, \mathbf{g}_1\rangle_\Gamma, \tag{6}$$

together with $\langle \mathbf{f}, \mathbf{g}\rangle_\Gamma := \int_\Gamma (\mathbf{f} \times \mathbf{n}) \cdot \mathbf{g}\, ds$. Note that on the discrete level we still need to compute the transmission matrix $\mathcal{A}(\omega)$ for each frequency ω, but the solution of the matrix equation is much easier because we are now using a drastically reduced resonance mode space.

The second approach for computing $\alpha_j(\omega)$ is based on a local approximation of the resolvent $\mathcal{A}(\omega)^{-1}$ by its principal part (PP) and has been proven particularly successful for plasmonic nanoparticles [12–14]. The starting point is Eq. (5), but we now choose as test functions the eigenfunctions $\tilde{\mathfrak{u}}_1, \ldots, \tilde{\mathfrak{u}}_J$ of the adjoint eigenvalue problem of the operator $\mathcal{A}(\omega)$, where the adjoint is considered with respect to the pairing $\langle \cdot, \bar{\cdot}\rangle$, as detailed in Ref. [26]. We then obtain instead of Eq. (5) the expression

$$\sum_{j=1}^{J} \alpha_j^{\mathrm{PP}}(\omega)\langle \mathfrak{u}_j, \overline{\mathcal{A}(\omega)^*\tilde{\mathfrak{u}}_\ell}\rangle = \langle \mathfrak{u}^{\mathrm{inc}}, \overline{\tilde{\mathfrak{u}}_\ell}\rangle, \tag{7}$$

where $\mathcal{A}(\omega)^*$ denotes the adjoint operator of $\mathcal{A}(\omega)$. We next follow Ref. [13] and assume that close to a resonance ω_ℓ,

$$\langle \mathfrak{u}_j, \overline{\mathcal{A}(\omega)^*\tilde{\mathfrak{u}}_\ell}\rangle \approx 0 \quad \text{for } j \neq \ell. \tag{8}$$

Strictly speaking, the term on the left-hand side is zero only for $\omega = \omega_\ell$, but one can expect that Eq. (8) also provides a good approximation close to the resonance. For the diagonal term, we expand the transmission operator in a Taylor series,

$$\mathcal{A}(\omega) \approx \mathcal{A}(\omega_\ell) + \left(\frac{d\mathcal{A}(\omega)}{d\omega}\right)_{\omega=\omega_\ell} (\omega - \omega_\ell), \tag{9}$$

and keep the linear term only. With this we get

$$\alpha_\ell^{\mathrm{PP}}(\omega) = \frac{1}{\omega - \omega_\ell} \frac{\langle \mathfrak{u}^{\mathrm{inc}}, \overline{\tilde{\mathfrak{u}}_\ell}\rangle}{\langle \mathcal{A}'(\omega_\ell)\mathfrak{u}_\ell, \overline{\tilde{\mathfrak{u}}_\ell}\rangle} + h_\ell(\omega), \tag{10}$$

with the prime in $\mathcal{A}'(\omega_\ell)$ denoting the derivative with respect to ω. $h_\ell(\omega)$ is a holomorphic function within the neighborhood of ω_ℓ which accounts for contributions not captured by

the resonance denominator of Eq. (10). Normalizing $\mathbf{u}_\ell$ such that $\langle \mathcal{A}'(\omega_\ell)\mathbf{u}_\ell, \overline{\tilde{\mathbf{u}}_\ell}\rangle = 1$ leads us to our final expression,

$$\mathbf{u}^{\mathrm{PP}} = \sum_{j=1}^{J} \frac{\langle \mathbf{u}^{\mathrm{inc}}, \overline{\tilde{\mathbf{u}}_j}\rangle}{\omega - \omega_j}\mathbf{u}_j, \tag{11}$$

where we have neglected the holomorphic contributions. The right-hand side accounts for the contribution of the principle part of $\mathcal{A}(\omega)^{-1}$ to the solution $(\mathbf{e}, \mathbf{h})$ in a neighborhood of the eigenvalues ω_j under consideration, in accordance to Keldysh's theorem [30].

Before pondering the results of resonance modes, it is important to realize that the approach is based on essentially two independent approximations. The first one concerns the resonance modes themselves, which are computed from Eq. (3), and the number of modes kept in the computation. The second approximation concerns the calculation of the expansion coefficients, using either the Galerkin approach of Eq. (5) or the principal value approach of Eq. (11). As we will demonstrate in the following, the choices for modes and coefficients are uncritical for structures with a strongly resonant behavior where only a few modes suffice for an excellent approximation, but things become considerably more complicated for larger nanoparticles whose response is governed by a larger number of resonances.

Boundary element method.—For the numerical solution of the matrix eigenvalue problem of Eq. (3), we use the contour integral method as given in Ref. [31]; see also Refs. [32,33]. The contour integral method is a reliable method for the approximation of all eigenvalues which lie inside of a given contour in the complex plane, and for the approximation of the corresponding eigenvectors. It is based on the contour integration of the resolvent $A(\omega)^{-1}$ and utilizes that the eigenvalues are poles of the resolvent. By contour integration of the resolvent, a reduction of the nonlinear eigenvalue problem to an equivalent linear eigenvalue problem is possible such that the eigenvalues of the linear problem coincide with those of the nonlinear one. In the Supplemental Material [26] we describe the basic ideas and the main steps of our algorithm for the numerical solution of the eigenvalue problem.

In our BEM approach we use a conforming Galerkin boundary element method with Raviart-Thomas elements of lowest order for the approximation of the integral operators, the eigenfunctions, and the reference solutions of the transmission problems. The modal approximations in the numerical examples are performed on the discrete level with the discrete counterparts of the operators and functions. For the computations of the boundary element matrices the open-source library BEM++ [34] is employed. The derivative $\mathcal{A}'(\omega)$ in Eq. (10) is approximated by a difference quotient. The required eigenvectors $\tilde{\mathbf{u}}_j$ in Eq. (10) of the adjoint problem coincide with $\mathbf{u}_j$ as shown in Ref. [26]. In all simulations we consider gold nanoparticles with a Drude permittivity taken from Refs. [13,14], and an refractive index of 1.5 for the background medium. We emphasize that the computation of the resonance modes is considerably more favorable for our BEM approach than for related FEM or FDTD schemes [12–14,16] because we are confronted neither with solutions diverging at infinity (all quantities are matched at the interface) nor with related difficulties regarding absorption in the perfectly matched layers.

We start by considering in complete analogy to Refs. [12,14] single and coupled nanocylinders, with dimensions detailed in the caption of Fig. 1. As can be seen in the figure, for the single cylinder only one resonance mode suffices to provide excellent extinction and scattering spectra within a broad frequency range. Similarly, for the coupled cylinders a reasonable approximation can be achieved for two modes, which are depicted in the Supplemental Material [26], although in this case we already observe deviations from the full simulation results.

Things change considerably for a simple nanosphere. As shown in the left-hand panel of Fig. 2 for the smallest sphere with a diameter of 50 nm, a single, threefold degenerate resonance suffices to obtain an excellent approximation of the optical spectra within the entire frequency regime. However, for the larger spheres we see noticeable deviations between the full simulations and the mode approximations

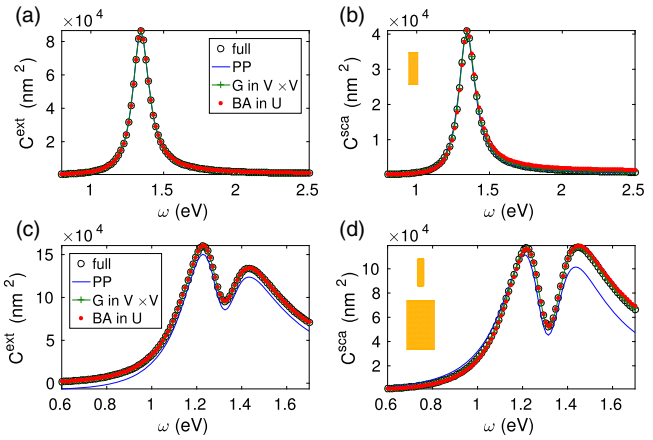

FIG. 1. (a),(b) Extinction C^{ext} and scattering C^{sca} cross sections for nanocylinder. A threefold degenerate resonance mode is used for the modal approximations. (c),(d) C^{ext} and C^{sca} for a dimer of two nanocylinders, with two modes for the modal approximations. Black open circles represent the results of the full BEM solutions, the blue line (PP) those of the approximation of the resolvent by its principle part, the green line (G in $V \times V$) those of the Galerkin approximation in $\mathbf{V} \times \mathbf{V}$, and the red dots (BA in U) those of the best approximation with respect to L^2-norm of the reference solution in $\mathcal{U}$. The single nanocylinder has a length of $d = 30$ nm and height of $h = 100$ nm, in complete analogy to Refs. [12,14]. The cylinder dimer has a gap of 45 nm, diameters of $d_1 = 20$ and $d_2 = 85$ nm, and heights of $h_1 = 80$ nm and $h_2 = 145$ nm, respectively. The cylinders are oriented along their long axes z, and we consider a plane wave excitation with a polarization along z.

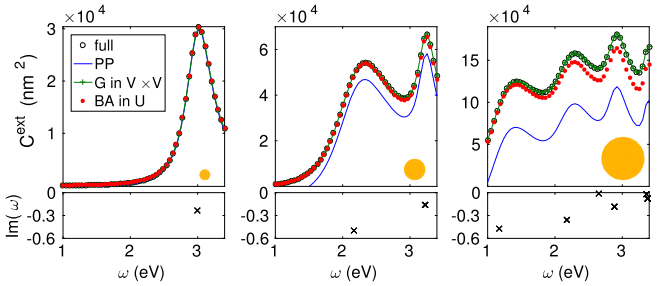

FIG. 2. Extinction cross sections for nanospheres with different diameters (upper plots) and distribution of the used resonances in the complex plane (black crosses in lower plots). The sphere diameters are $d = 50$ nm (left), 100 nm (middle), and 200 nm (right), and the number of modes are 3, 8, and 18.

PP, with unacceptably large errors for the largest sphere. To evaluate whether these errors are due to a limited basis or the calculation scheme for the expansion coefficients, in the following we introduce a "best approximation" (BA), which we obtain by first computing the full tangential fields $\mathbf{e}, \mathbf{h}$ and then obtaining from Eq. (4) the best coefficients using a least-squares fit. Comparing the black open and filled red symbols in Fig. 2, we observe that the best approximation is considerably better than the principal part approximation, although for the largest sphere the deviations between the two spectra are still surprisingly large. Similar findings as for the sphere are made for the cube; see Fig. 3. We refrain from showing results obtained from the Galerkin approximation in $\mathcal{U}$, see Eq. (5), since they are significantly worse.

In what follows, we first analyze the shortcomings of the usual PP scheme within the framework of Mie theory, which provides analytic results for spherical nanoparticles, and then suggest a novel modal approximation scheme, which we denote as G in $V \times V$ for reasons to become clear in a moment. As can be seen in all figures, this novel scheme dramatically outperforms the PP one and gives excellent agreement with the full simulation results throughout.

Mie theory.—For the case of a sphere we employ the framework of Mie theory and expand the electromagnetic fields using vector spherical harmonics and match the fields

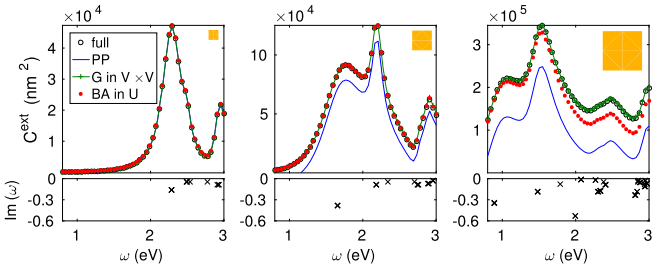

FIG. 3. Extinction cross sections for nanocubes with different side lengths (upper plots) and distribution of the used resonances in the complex plane (black crosses in lower plots). The lengths of the cubes are $a = 50$ nm (left), 100 nm (middle), and 200 nm (right), and the number of modes are 14, 25, and 54.

at the sphere boundary [35]. The full derivation can be found in Ref. [26]. In short, we obtain two types of modes, namely the transverse magnetic $\mathbf{e}_{nm}^{\mathrm{TM}}$, $\mathbf{h}_{nm}^{\mathrm{TM}}$ and transverse electric $\mathbf{e}_{n}^{\mathrm{TE},m}$, $\mathbf{h}_{n}^{\mathrm{TE},m}$ ones. Here, n and m denote the spherical degree and order, respectively. Let k_n^{TM} and k_n^{TE} denote the eigenvalues for these two modes, respectively. The Mie solutions can then be expressed in the form [see also Eq. (18) of SM [26]]

$$\mathbf{e} = \sum_{n,m}\left[a_n^m \frac{\mathcal{I}_{e,n}^{\mathrm{TM}}(k_1 R)}{\mathcal{I}_{e,n}^{\mathrm{TM}}(k_n^{\mathrm{TM}} R)}\mathbf{e}_{nm}^{\mathrm{TM}} + b_n^m \frac{\mathcal{I}_{e,n}^{\mathrm{TE}}(k_1 R)}{\mathcal{I}_{e,n}^{\mathrm{TE}}(k_n^{\mathrm{TE}} R)}\mathbf{e}_{nm}^{\mathrm{TE}}\right],$$
$$\mathbf{h} = \sum_{n,m}\left[a_n^m \frac{\mathcal{I}_{h,n}^{\mathrm{TM}}(k_1 R)}{\mathcal{I}_{h,n}^{\mathrm{TM}}(k_n^{\mathrm{TM}} R)}\mathbf{h}_{nm}^{\mathrm{TM}} + b_n^m \frac{\mathcal{I}_{h,n}^{\mathrm{TE}}(k_1 R)}{\mathcal{I}_{h,n}^{\mathrm{TE}}(k_n^{\mathrm{TE}} R)}\mathbf{h}_{nm}^{\mathrm{TE}}\right], \quad (12)$$

where $\mathcal{I}_{e,h}$ are functions that depend on the spherical Bessel function j_n and their derivatives, associated with the radial parts of the modes, and a, b are the usual Mie coefficients. The important point about Eq. (12) is that for both TM and TE modes the expansion coefficients for $\mathbf{e}$ and $\mathbf{h}$ (in terms of the resonance modes $\mathbf{e}_{nm}$ and $\mathbf{h}_{nm}$) only coincide at the complex eigenfrequencies but are different otherwise. Thus, tying together the electric and magnetic fields in one vector $\mathbf{u} = (\mathbf{e}_j, \mathbf{h}_j)$, as we have previously done in accordance to the prescriptions given in the literature [12–14], is not supported by our Mie analysis.

Novel modal decomposition.—We finally suggest a modal approach which allows different coefficients for the electric and magnetic field components. We start from the previously computed resonance modes but enlarge our modal space using

$$\mathbf{V} \times \mathbf{V} \coloneqq \mathrm{span}\left\{\begin{pmatrix}\mathbf{e}_j\\ \mathbf{0}\end{pmatrix}, \begin{pmatrix}\mathbf{h}_j\\ \mathbf{0}\end{pmatrix}, \begin{pmatrix}\mathbf{0}\\ \mathbf{e}_j\end{pmatrix}, \begin{pmatrix}\mathbf{0}\\ \mathbf{h}_j\end{pmatrix}\right\}_{j=1}^{J},$$

together with a suitable procedure (such as a singular value decomposition) in order to remove linearly dependent vectors from the new space. Note that $\mathbf{e}_j$, $\mathbf{h}_j$ are both tangential fields on the boundary and can thus be safely mixed together. With the above choice we can unfortunately no longer use a simple prescription similar as in Eq. (11) for the computation of the expansion coefficients, but must resort to a Galerkin scheme as in Eq. (5). The symbols denoted with G in Figs. 1–3 show the results of such calculations. Remarkably, we obtain excellent agreement with the full results throughout.

Our results are encouraging as they show that the resonance modes themselves suffice to provide excellent agreement with full simulations even for relatively large structures. As the modes are computed without making any specific assumptions about the external excitation, our approach can not only be used for plane wave excitations, as we have done for simplicity in this work, but can be immediately adapted to other excitation sources, such as oscillating dipoles or swift electrons, as used in electron

energy loss spectroscopy. The major shortcoming of our approach is that the transmission matrix $\mathcal{A}(\omega)$ still needs to be computed for every frequency, although the solution of the transmission problem in the subspace of resonance modes is drastically reduced with respect to full simulations. We have tried to generalize the approach of Eq. (11) for separate electric and magnetic field components, but have not yet found a satisfying solution scheme. Ideally, the computation of the coefficients should invoke only the resonance frequencies and modes, as well as the incoming fields. Whether such an approach is possible will be the subject of future work.

This work has been supported in part by the Austrian science fund FWF under the SFB F49 NextLite (F4906-N23), Project No. P27299–N27, and NAWI Graz.

*ulrich.hohenester@uni-graz.at

[1] W. L. Barnes, A. Dereux, and T. W. Ebbesen, Nature (London) **424**, 824 (2003).
[2] M. I. Stockman, Opt. Express **19**, 22029 (2011).
[3] A. Trügler, *Optical Properties of Metallic Nanoparticles: Basic Principles and Simulation* (Springer, Berlin, 2015).
[4] J. A. Schuller, E. S. Barnard, W. Cai, Y. C. Jun, J. S. White, and M. L. Brongersma, Nat. Mater. **9**, 193 (2010).
[5] R. Fuchs, Phys. Rev. B **11**, 1732 (1975).
[6] F. Ouyang and M. Isaacson, Philos. Mag. B **60**, 481 (1989).
[7] G. Boudarham and M. Kociak, Phys. Rev. B **85**, 245447 (2012).
[8] A. Hörl, A. Trügler, and U. Hohenester, Phys. Rev. Lett. **111**, 076801 (2013).
[9] O. Nicoletti, F. de la Pena, R. W. Leary, D. J. Holland, C. Ducati, and P. A. Midgley, Nature (London) **502**, 80 (2013).
[10] H. Lourenco-Martins, P. Das, L. H. G. Tizei, R. Weil, and M. Kociak, Nat. Phys. **14**, 360 (2018).
[11] P. T. Leung, S. Y. Liu, and K. Young, Phys. Rev. A **49**, 3057 (1994).
[12] Q. Bai, M. Perrin, C. Sauvan, J.-P. Hugonin, and P. Lalanne, Opt. Express **21**, 27371 (2013).
[13] C. Sauvan, J. P. Hugonin, I. S. Maksymov, and P. Lalanne, Phys. Rev. Lett. **110**, 237401 (2013).
[14] M. Perrin, Opt. Express **24**, 27137 (2016).
[15] P. T. Kristensen, C. Van Vlack, and S. Hughes, Opt. Lett. **37**, 1649 (2012).
[16] R. C. Ge, P. T. Kristensen, J. F. Young, and S. Hughes, New J. Phys. **16**, 113048 (2014).
[17] M. B. Doost, W. Langbein, and E. A. Muljarov, Phys. Rev. A **90**, 013834 (2014).
[18] E. A. Muljarov and W. Langbein, Phys. Rev. B **93**, 075417 (2016).
[19] J. Mäkitalo, M. Kauranen, and S. Suuriniemi, Phys. Rev. B **89**, 165429 (2014).
[20] Y. Chang and R. Harrington, IEEE Trans. Antennas Propag. **25**, 789 (1977).
[21] A. J. Poggio and E. K. Miller, in *Computer Techniques for Electromagnetics*, International Series of Monographs in Electrical Engineering, edited by R. Mittra (Pergamon, New York, 1973), pp. 159–264.
[22] T. K. Wu and L. L. Tsai, Radio Sci. **12**, 709 (1977).
[23] A. Buffa, R. Hiptmair, T. von Petersdorff, and C. Schwab, Numer. Math. **95**, 459 (2003).
[24] A. Buffa and R. Hiptmair, *Topics in Computational Wave Propagation*, Lecture Notes in Computational Science and Engineering Vol. 31 (Springer, Berlin, 2003), pp. 83–124.
[25] G. Unger, Institute of Computational Mathematics, Graz University of Technology Report No. 2017/2, 2017.
[26] See Supplemental Material at http://link.aps.org/supplemental/10.1103/PhysRevLett.121.246802 for details on the derivation of the boundary integral formulation, the calculation of the fields and the cross sections, the analytical expansion on the sphere, the characterization of the adjoint modes, and the contour integral method, which includes Refs. [27,28].
[27] S. Benghorieb, R. Saoudi, and A. V. Tishchenko, Plasmonics **6**, 445 (2011).
[28] A. Kirsch and F. Hettlich, *The Mathematical Theory of Time-Harmonic Maxwell's Equations: Expansion-, Integral-, and Variational Methods* (Springer, New York, 2014).
[29] R. Mennicken and M. Möller, *Non-Self-Adjoint Boundary Eigenvalue Problems* (North-Holland Publishing Co., Amsterdam, 2003).
[30] V. Kozlov and V. Maz'ya, *Differential Equations with Operator Coefficients with Applications to Boundary Value Problems for Partial Differential Equations* (Springer, Berlin, 1999).
[31] W.-J. Beyn, Linear Algebra Appl. **436**, 3839 (2012).
[32] J. Asakura, T. Sakurai, H. Tadano, T. Ikegami, and K. Kimura, J. SIAM Lett. **1**, 52 (2009).
[33] S. Yokota and T. Sakurai, J. SIAM Lett. **5**, 41 (2013).
[34] W. Śmigaj, S. Arridge, T. Betcke, J. Phillips, and J. Schweiger, ACM Trans. Math. Softw. **41**, 1 (2015).
[35] C. Bohren and D. R. Huffman, *Absorption and Scattering of Light by Small Particles*, in Wiley Science Paperback Series (Wiley-VCH Verlag, New York, 1983).